Biophysical Chemistry 135 (2008) 25–31

Contents lists available at ScienceDirect

Biophysical Chemistry

journal homepage: http://www.elsevier.com/locate/biophyschem

Salts enhance both protein stability and amyloid formation of an immunoglobulin light chain

Laura A. Sikkink, Marina Ramirez-Alvarado *

Department of Biochemistry and Molecular Biology, College of Medicine, Mayo Clinic 200 First Street SW, Rochester, MN 55905 USA

ARTICLE INFO

Article history:
Received 24 January 2008
Received in revised form 29 February 2008
Accepted 29 February 2008
Available online 18 March 2008

Keywords:
Amyloid
Protein stability
Hofmeister salts
Immunoglobulin light chain
Light Chain Amyloidosis

ABSTRACT

Amyloid fibrils are associated with sulfated glycosaminoglycans in the extracellular matrix. The presence of sulfated glycosaminoglycans is known to promote amyloid formation *in vitro* and *in vivo*, with the sulfate groups playing a role in this process. In order to understand the role that sulfate plays in amyloid formation, we have studied the effect of salts from the Hofmeister series on the protein structure, stability and amyloid formation of an amyloidogenic light chain protein, AL-12. We have been able to show for the first time a direct correlation between protein stability and amyloid formation enhancement by salts from the Hofmeister series, where SO_4^{2-} conferred the most protein stability and enhancement of amyloid formation. Our study emphasizes the importance of the effect of ions in the protein bound water properties and downplays the role of specific interactions between the protein and ions.

1. Introduction

Light Chain Amyloidosis (AL) is a protein misfolding disease caused by an abnormal proliferation of monoclonal plasma B cells that secrete free Light Chains (LC) into circulation. These free LC misfold and aggregate as amyloid fibrils in vital organs, causing organ failure and death. Somatic mutations are the most studied source of LC destabilization causing the protein to sample partially unfolded states that lead to amyloid formation. These amino acid substitutions have a global destabilizing effect, so that less energy is required to unfold the protein [1–3]. The propensity to form amyloid fibrils *in vitro* correlates with a decrease in folding stability for some AL proteins, suggesting that destabilizing interactions influence the kinetics of amyloid formation [4].

Amyloid fibril formation studies with AL proteins have been performed under non-physiological conditions, such as low pH for the variable domain (VL) protein 'SMA' and by addition of Na_2SO_4 in combination with incubation at the melting temperature (T_m) for the VL protein 'AL-09' [5–9]. Na_2SO_4 has been used to promote amyloid fibril formation with a number of amyloid-related and unrelated protein precursors, including AL-09, protein G B1 variant I6T53 and β2-microglobulin [9–11].

The determinants of amyloid formation and the role external factors play in this process are not well understood. In particular, little is known about the role and nature of the influence SO_4^{2-} plays in stabilizing folded states, folding intermediates and promoting amyloid formation. SO_4^{2-} is relevant to amyloid deposition *in vivo* because glycosaminoglycans (GAGs) are sulfated heterogeneous polysaccharides composed of repeating disaccharide units of glucuronic or iduronic acid and *N*-acetylglucosamine or *N*-acetylgalactosamine [12,13]. Several groups have shown that GAGs promote and stabilize amyloid fibril formation and deposition *in vitro* and *in vivo* [14–16]. It is thought that the multiple negative charges from the SO_4^{2-} ions present in these macromolecules are an important factor in promoting amyloid formation in the extracellular matrix [17].

In 1888, Lewith and Hofmeister published accounts of great differences between the minimum concentrations of various neutral salts required to precipitate a given protein from solution [18]. The results are compiled into what it is now known as the Hofmeister series, where various ions are ordered according to their effectiveness in promoting protein stability and solubility. The underlying concept is that interactions between biopolymers in aqueous media are mediated by water; cosolutes such as neutral salts can influence both the surfaces of the solid bodies and the structure of the water. The Hofmeister series includes kosmotropic ions that interact strongly with water and stabilize proteins by promoting stronger interactions among non-polar groups (salting-out) and chaotropic ions that destabilize proteins by breaking hydrogen bonds within the peptide groups (salting-in) [19]. Baldwin reports data from Jarvis and Scheiman [30] showing that surface tension of salt solutions follows the rank order of the Hofmeister series [19]. The surface tension increases with salt concentration. Work by Nandi and Robinson in 1972 [31], also reviewed by Baldwin showed that salting-out constants are proportional to the accessible surface area of the amino acid used. These salting-out constants are proportional to the surface tension

* Corresponding author. Tel.: +1 507 284 2705; fax: +1 507 284 9759.
E-mail address: ramirezalvarado.marina@mayo.edu (M. Ramirez-Alvarado).

0301-4622/$ – see front matter © 2008 Elsevier B.V. All rights reserved.
doi:10.1016/j.bpc.2008.02.019

increments of the salts, suggesting that these physical properties of the solutions are not protein specific. James Hallewell St. Johnston reported in 1927 that the surface tension of Na_2SO_4 albumin and caseinogen solutions changed following the same pattern [20]. $NaNO_3$ and NaCl caseinogen solutions increased surface tension as a function of salt concentration, but to a lesser extent compared to Na_2SO_4, in agreement with Jarvis and Scheiman [30]—reviewed in [19]. Baldwin concludes that Hofmeister interactions are unusual because they show a similar pattern, not only with different globular proteins but with DNA and collagen. The Hofmeister series is dominated by anions, with Cl^- having little effect even at high concentrations and being considered a null (middle) point where the opposite interactions (salting-in and salting-out) cancel out. SO_4^{2-} is among the most stabilizing of the anions described in the Hofmeister series. Experimentally, SO_4^{2-} confers thermodynamic stability in multiple systems, including AL-09 and prion proteins [9–22]. Other anions besides SO_4^{2-} have also been shown to affect the formation of fibrils for other amyloid precursors. Anions induce partial folding of the natively unfolded α-synuclein, forming a critical amyloidogenic intermediate that leads to the acceleration of the rate of fibrillation. The magnitude of acceleration correlated with the position of anions in the Hofmeister series [23]. Salts have an effect on the aggregation of Aβ(1-40) amyloid fibrils by promoting different degrees of nucleation and growth [24]. Klement et al. reported little effect of salts on the freshly dissolved unfolded Aβ(1-40) but they demonstrated strong effect on the fibrillar peptide. It is possible that salts affect amyloid precursor proteins that are natively folded in different ways that they affect small unfolded polypeptides, such as Aβ(1-40). The effect of SO_4^{2-} and other anions in amyloid precursor proteins with a folded conformation may possibly shift from salting-out stabilizing effects to salting-in destabilizing effects during the aggregation process. We are interested in understanding this role and correlating these effects to the sulfated glycosaminoglycans promoting amyloid formation.

We conducted a proof of principle study in which we tested the effect of physiologically relevant anions and cations on AL-12 protein structure, thermodynamic stability and amyloid formation. The salts tested did not affect protein structure. Thermodynamic stability and amyloid formation were enhanced according to the rankings of the Hofmeister series. The largest enhancement was seen with SO_4^{2-} anions and Mg^{2+} cations.

2. Materials and methods

2.1. Cloning/expression/extraction/purification

Patient AL-12 presented with cardiac AL. AL-12 VL sequence was previously deposited in GenBank (the first amino acid begins at nucleotide 51 and ends with nucleotide 374) with the accession number AF490912 [25]. Upon resequencing, we confirmed that codon 88 corresponded to cysteine. cDNA was created according to the methods in Abraham et al. [25]. Briefly, RNA was extracted from bone marrow and cDNA was produced by RT-PCR and cloned into the pCR®II-TOPO® cloning vector (Invitrogen, Carlsbad, CA). The DNA was then subcloned into the pET12a vector (Novagen, Madison, WI). The plasmid was transformed into BL21 (DE3) Gold competent cells (Stratagene, La Jolla, CA) and protein expression was induced with 0.8 mM IPTG (isopropyl-beta-D-thiogalactopyranoside). After 17–20 h of post induction growth, the bacteria were collected, pelleted and frozen. Protein was extracted from the periplasmic space of the bacteria with a freeze–thaw step followed by osmotic shock using 20% sucrose in 10 mM Tris HCl pH 9.0 and eluted with 10 mM Tris HCl pH 9.0. The periplasmic fraction was then dialyzed into 10 mM Tris HCl pH 7.4. The protein was purified using size exclusion chromatography (HiLoad 16/60 Superdex 75 column) on an AKTA FPLC (GE Healthcare, Piscataway, NJ). Pure fractions were checked by SDS polyacrylamide gel electrophoresis (SDS-PAGE) and stained with Coomassie Blue. A Western Blot was used to confirm the purified protein identity by using a sheep anti human kappa light chain as the primary antibody (The Binding Site Inc., San Diego, CA). The secondary antibody was a rabbit anti sheep polyclonal IgG H & L (HRP) antibody (Abcam Inc., Cambridge, MA). Protein concentration was determined by its absorbance at 280 nm, the calculated extinction coefficient and the cuvette pathlength. The extinction coefficient of 13,610 $(M\ cm)^{-1}$ was calculated using the peptide property calculator (www.basic.northwestern.edu/biotools/proteincalc.html) and the protein sequence. Pure fractions were combined, concentrated, flash frozen and stored at −20 °C.

2.2. Analytical size exclusion chromatography

The oligomeric state of the purified protein was determined on a Superdex 75 10/30 size exclusion column on an AKTA FPLC (GE Healthcare, Piscataway, NJ). Albumin, carbonic anhydrase, cytochrome *C* and aprotinin (Sigma, St. Louis, MO) were used as molecular weight standards. Each standard was prepared in 10 mM Tris HCl pH 7.4, 0.15 M NaCl. The column was calibrated with each standard at a flow rate of 0.3 ml/min. The elution volume for each standard peak was determined. Blue dextran was injected onto the column to determine its void volume, which was used to calculate the ratio of elution to void volume (Ve/Vo) for each molecular weight standard. A calibration curve was produced by plotting the logarithm of molecular weight standards as a function of their Ve/Vo and determining the line of best fit. The purified AL-12 was injected and eluted through the column at a flow rate of 0.3 ml/ min in the same buffer as the standards. After determining the Ve/Vo of AL-12, the molecular weight was calculated by using the equation for the line of best fit.

2.3. Circular dichroism spectroscopy (CD)

Secondary structure of AL-12 was measured by following the Far UV-CD spectrum (Jasco Spectropolarimeter 810, JASCO Inc, Easton, MD) from 260–200 nm, taking measurements every 1 nm with a scanning speed of 10 nm/ min at 4 °C in a 0.2 cm cuvette. Protein concentration was 20 μM. Samples were done triplicate with the average of the 3 scans reported. Individual samples for ionic strength of 1 were analyzed. Secondary structure of AL-12 ± 0.5 M Na_2SO_4 at various temperatures were followed by Far UV-CD in a 0.1 cm cuvette following the same parameters listed above. Samples were incubated at each temperature for 15 min prior to the Far UV-CD scan.

Thermal denaturation experiments were done by following ellipticity at 216 nm, from 4–90 °C every 2 °C with a temperature slope of 30 °C/h and response time of 32 s. Refolding data were acquired immediately after the unfolding curve from 90–4 °C using the same parameters listed above. Thermal denaturation data was processed following a two-state transition model. Folded and unfolded baselines were linearly extrapolated from the data with a minimum of 10 points. The fraction folded (FF) at each temperature was calculated by using the following equation: FF = (ellipticity observed − ellipticity of the unfolded)/(ellipticity of folded − ellipticity of unfolded). The T_m was calculated at the temperature in the midpoint transition where 50% of the protein was folded. Solutions of AL-12 (20 μM) in the presence of various salts (Na_2SO_4, NaCl, $MgSO_4$, $MgCl_2$, NH_4Cl, Na_2HPO_4) at a concentration of 0.5 M were prepared and allowed to equilibrate overnight at 4 °C before acquisition of CD data. Samples were done in triplicate. ANOVA single factor analysis was done using the T_m of the various salts to determine the *p*-values.

A chemical denaturation experiment was done by equilibrating individual samples of AL-12 (20 μM) with various urea concentrations (0–6 M) for 42 h at 4 °C. Parameters previously described were used to acquire the Far UV-CD spectra from 260–200 nm. The ellipticity at 212 nm was used as a function of urea concentration because it provided the greatest difference between 0–6 M urea. Each urea concentration was verified using refractometry and calculated using the following equation: $[\text{urea}] = 117.66 * \Delta N + 29.753 * B(\Delta N)^2 + 185.56 * (\Delta N)^3$, where ΔN is the difference in refraction between each sample and buffer

[26]. The denaturation curves were processed the same way as the two-state transition model used in the thermal denaturation to calculate fraction folded curves. The melting concentration of denaturant (C_m) was determined at the urea concentration where 50% of the protein was folded. $\Delta G_{folding}$ was calculated using the following equation: $\Delta G_{folding} = -RT\ln Keq$ ($R = 1.98$ cal mol^{-1} K^{-1}, T = temperature in Kelvin, Keq = equilibrium constant of folding ([folded]/[unfolded]) derived from chemical denaturation data) [26].

2.4. Fibril formation

20 μM AL-12 in 10 mM Tris HCl pH 7.4 and 5 μM Thioflavine T (ThT) with 0.5 M salts (Na_2SO_4, NaCl, $MgSO_4$, $MgCl_2$, NH_4Cl, Na_2HPO_4, a combination of 0.25 M NaCl, 0.25 M Na_2SO_4 and 0.15 M NaCl, 0.35 M Na_2SO_4) were incubated in a microcentrifuge tube at their T_m (59 °C for SO_4^{2-}, 52 °C for Cl^-, 59 °C for Cl^-, SO_4^{2-}, 55 °C for NH_4^+) for 28–118 h with constant agitation at 300 rpm. Each sample was set up in triplicate. At various time points, 100 μl of each sample was checked on a PTI-QM2001 fluorometer (Photon Technology International, Lawrenceville, NJ) using an excitation wavelength of 450 nm following emission from 470–530 nm. Fibril formation samples were centrifuged and the supernatant was collected and its absorbance at 280 nm was determined on a UV/Vis spectrophotometer (Molecular Devices, Sunnyvale, CA) to determine the concentration of the remaining protein to calculate amyloid fibril yield. The concentration of fibrils was determined by subtracting the supernatant concentration from the starting protein concentration. We used this method to calculate percent protein incorporated in fibrils for Fig. 3E.

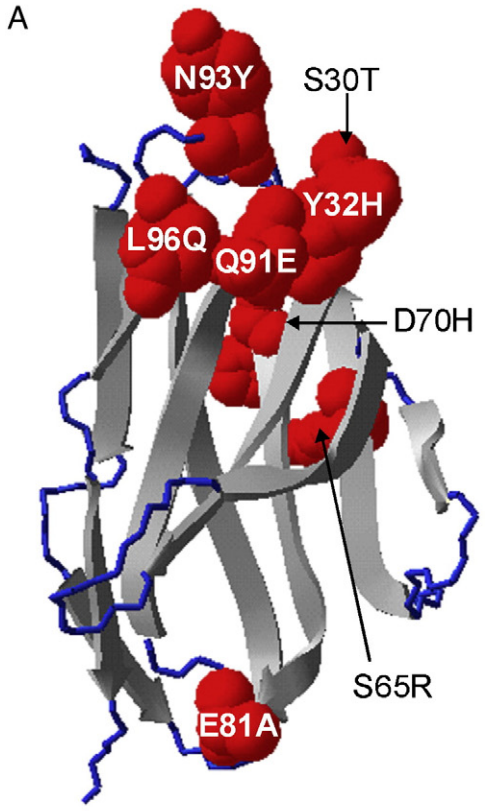

B

Mutation	Location
S30T	CDR1
Y32H	Dimer Interface strand C
S65R	β–Hairpin (strand D)
D70H	β–Hairpin (strand E)
E81A	Loop between E and F
Q91E	Dimer Interface strand F
N93Y	CDR3
L96Q	FR4

Fig. 1. A. Model of AL-12 based on the 1BRE.pdb crystal structure showing the location of each mutation in AL-12. Mutations are shown in red, β sheets are in gray and loops are in blue. B. Description of the locations of mutations.

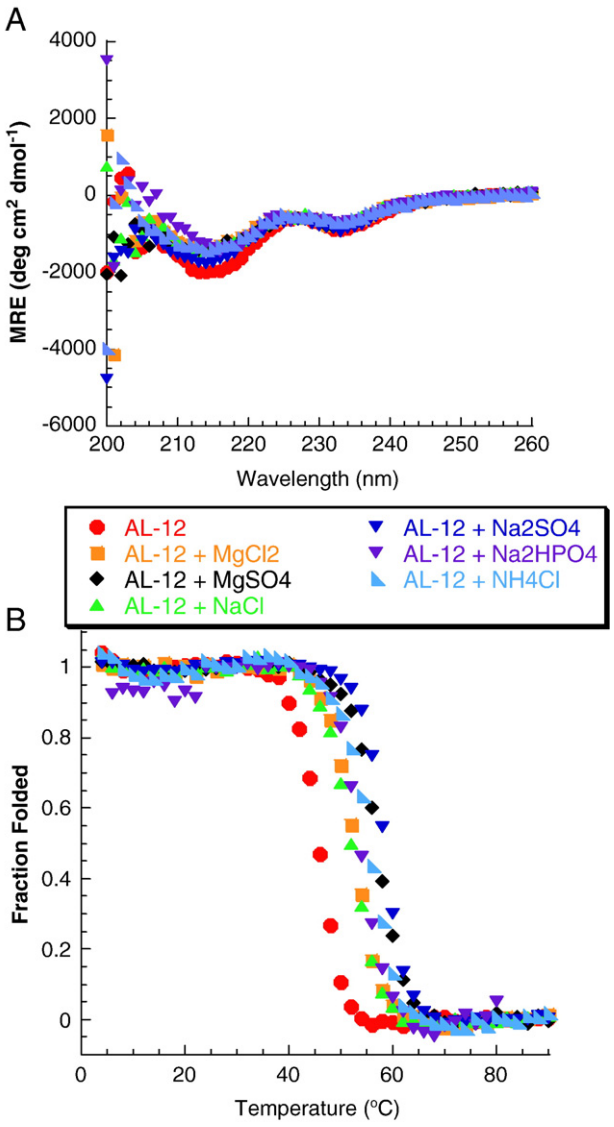

Fig. 2. A. AL-12 has a β sheet conformation by Far UV-CD in the presence and absence of various salts. All Far UV-CD scans were performed at 4 °C and are the average of three separate samples. B. AL-12 has different thermodynamic stability in the presence of various salts. Thermal denaturation experiments were followed at 216 nm. Experimental conditions: 10 mM Tris HCl pH 7.4 buffer ±0.5 M salt, 20 μM protein.

2.5. Electron microscopy (EM)

Fibrils (pellets) were washed three times with 10 mM Tris HCl pH 7.4, 0.02% NaN_3 buffer. 3 μl of each washed fibril sample was placed on a 300 mesh copper formvar/carbon grid and air dried. Grids were

negatively stained with 4% uranyl acetate, washed, air dried and examined on either a JEOL 1200 EX or Philips Tecnai T12 transmission electron microscope.

3. Results

AL-12 VL sequence belongs to the κI O18/O8 germline and has 8 somatic mutations which include S30T, *Y32H*, *S65R*, *D70H*, *E81A*, *Q91E*, *N93Y* and *L96Q* (Fig. 1). Seven of these somatic mutations are non-conservative (italics) and are located throughout the protein in the top of the β-barrel and the β-hairpin DE. Recombinant AL-12 (3.5 μM) is a monomer as determined from analytical size exclusion chromatography with a calculated molecular weight of 12,661 Da.

We first performed circular dichroism spectroscopy (CD) to determine the secondary structure of AL-12. The protein presents a β sheet structure by Far UV-CD with a minimum at 216 nm (Fig. 2A). The spectrum also has a slight minimum around 235 nm, which may be due to the contribution of the 11 aromatic residues present in AL-12 (1 tryptophan, 4 phenylanine, 6 tyrosine) [27]. This minimum has also been observed with AL-09, another light chain protein characterized in our laboratory [9]. The thermal denaturation of AL-12 suggests a two-state unfolding transition with a T_m of 46.1 °C±0.2 (Fig. 2B). AL-12 refolds reversibly (data not shown). Chemical denaturation data of AL-12 produced a melting concentration of urea (C_m) of 2.3 M and $\Delta G_{folding}$ of −3.6 kcal/mol (data not shown).

To determine the concentration of salts that confer maximum stability for AL-12, we acquired thermal denaturation data over a range of Na_2SO_4 concentrations (data not shown). The thermodynamic stabilities between 0.5 and 0.6 M Na_2SO_4 were very similar with T_m values of 58.8 °C±0.5 and 59.8 °C±0.5 respectively. Precipitation occurred during thermal denaturation experiments between 0.7–1 M Na_2SO_4. Based on these results, 0.5 M Na_2SO_4 was chosen as the optimal salt concentration since it showed the maximum increase in thermodynamic stability while maintaining its solubility and was the concentration used for the rest of the salts studied.

Various anions (SO_4^{2-}, HPO_4^{2-}, Cl^-, NO_3^-, I^-, $C_6H_5O_7^{3-}$) and cations (NH_4^+, Na^+, Mg^{2+}) were chosen based on their different solubility and stability rankings in the Hofmeister series as well as their physiological relevance. $NaNO_3$, NaI, and $Na_3C_6H_5O_7$ were unable to be studied due to their large absorbance in the Far UV-CD region even at low salt concentrations (data not shown) so we focused our studies on the remaining salts. AL-12 retained its β sheet structure and showed a T_m increase from 5.1–13.2 °C in the presence of the different salts, with the largest T_m increase attributed to Na_2SO_4 followed closely by $MgSO_4$ (Fig. 2 and Table 1). All thermal denaturation data of AL-12 in the presence of different salts followed a two-state unfolding transition. Most reactions were able to refold reversibly with the exception of AL-12 with 0.5 M Na_2HPO_4, which precipitated at high temperatures (data not shown). The separate anions and cations studied showed the following stabilizing pattern for AL-12: $SO_4^{2-} > HPO_4^- > Cl^-$ and $NH_4^+ > Mg^{2+} \approx Na^+$ respectively. These stabilizing effects are in agreement with the Hofmeister series. These results demonstrate that different anions and cations can significantly affect the stability of AL-12 without affecting its secondary structure at the concentration studied. The *p*-values from the comparisons of the different salts T_m values showed that the T_m value differences are statistically significant (Supplemental Fig. 2).

Since the salts selected for our study have different ionic strengths at 0.5 M, we studied AL-12 protein structure and stability at different salt concentrations to adjust for an ionic strength of 1. The T_m values show smaller differences at ionic strength of 1 compared to the values at 0.5 M salt concentration. The ranking of cations ($NH_4^+ > Na^+ > Mg^{2+}$) and anions ($SO_4^{2-} > Cl^-$), as determined by their T_m values, follow the Hofmeister series. The cations play a larger role in protein stability at this ionic strength. AL-12 with 1 M NH_4Cl has the highest T_m (59.3 °C±0.5) (Supplementary Fig. 1, Table 1). AL-12 in the presence of 0.33 M Na_2HPO_4 was not able to refold reversibly at high temperatures due to precipitation.

We wanted to determine if the presence of two anions in solution, in particular Cl^- and SO_4^{2-}, would have competing, neutral or synergistic effects on protein stability based on an initial observation that 0.15 M NaCl, 0.5 M Na_2SO_4 appeared to have a synergistic effect on amyloid formation (data not shown). We studied AL-12 with 0.25 M NaCl, 0.25 M Na_2SO_4 and 0.15 M NaCl, 0.35 M Na_2SO_4. These dual anion samples did not affect the secondary structure of AL-12 and the T_m was 55.7 °C±0.5 for 0.25 M NaCl, 0.25 M Na_2SO_4, 55.5 °C±0.5 for 0.1 M NaCl, 0.30 M Na_2SO_4 and 56.9 °C±0.4 for 0.15 M NaCl, 0.35 M Na_2SO_4 (data not shown). These results suggest that increasing the concentration of Na_2SO_4 increases the stability of AL-12 regardless of the concentration of NaCl.

We analyzed the effects of various salts (Na_2SO_4, $MgSO_4$, NH_4Cl, NaCl, $MgCl_2$) on AL-12 fibril formation. In addition, AL-12 was incubated with 0.25 M NaCl, 0.25 M Na_2SO_4 or 0.15 M NaCl, 0.35 M Na_2SO_4 to determine if the presence of the two anions (SO_4^{2-} and Cl^-) had competing, neutral or synergistic effects in amyloid formation. Na_2HPO_4 was not included since it precipitates at high temperatures and interferes with our fibril formation experiments. We performed these experiments by incubating the protein at its T_m with continuous agitation to maximize amyloid formation as previously described [9–28]. All salts accelerated amyloid formation and greatly shorten the lag time (Fig. 3A,B,C,D). A large ThT fluorescence enhancement is usually directly correlated with the amount of fibrils in the reaction. Thioflavine T (ThT) fluorescence enhancement vary among the different salts which may be due to the large amounts of fibrils clustering and possibly causing inner filter effects or the stage of the reaction at a given point in time.

Electron microscopy (EM) of endpoint samples with different salts show fibrils in all the conditions, but with different degrees of clustering (Supplemental Fig. 3). This clustering may cause a reduction of the ThT fluorescence enhancement by blocking ThT binding sites on the fibrils due to a reduction in exposed surface area. In order to determine if clustering is affecting the ThT fluorescence enhancement readings, we proceeded to calculate the amount of protein incorporated in the fibrils by measuring the remaining protein concentration in the supernatant of each reaction to calculate amyloid fibril yield (Fig. 3E). The reactions with Mg2+ had the highest amyloid yield followed by the reactions with Na_2SO_4, NaCl and NH_4Cl. The presence of different amounts of Cl^- does not affect amyloid formation in the dual anion samples since their amyloid yields are similar within error. AL-12 alone incorporated the lowest percentage of protein into fibrils, in agreement with the slow lag time and the low ThT fluorescence enhancement. These results suggest that for certain reactions, ThT fluorescence enhancement may not reflect net amyloid formation due to the loss of signal caused by clustering of fibrils in the reaction. In our experiments, amyloid fibril yield measurement more truly reflects the amount of amyloid formed. In summary, a combination of lag time, ThT fluorescence enhancement and amyloid yield gives a more complete picture of the effect the various

Table 1
The effect of salts on the melting temperature (T_m) of AL-12 determined by CD

Sample	0.5 M salt concentration T_m ± standard deviation (°C)	Ionic strength at 0.5 M salt	Salt concentration at ionic strength of 1 (M)	Ionic strength of 1 T_m (°C)*
AL-12	46.1±0.2	NA	NA	NA
AL-12 + NaCl	51.9±0.6	0.5	1	54.5
AL-12 + $MgCl_2$	52.4±0.2	1.5	0.33	51.6
AL-12 + Na_2HPO_4	53.8±1.3	1.5	0.33	50.9
AL-12 + NH_4Cl	55.2±0.5	0.5	1	59.3
AL-12 + 0.25 M NaCl, 0.25 M Na_2SO_4	55.7±0.5	1.0	0.25, 0.25	55.7
AL-12 + 0.15 M NaCl, 0.35 M Na_2SO_4	56.9±0.4	1.2	0.10, 0.30	55.5
AL-12 + $MgSO_4$	57.1±0.1	2.0	0.25	53.8
AL-12 + Na_2SO_4	59.3±1.7	1.5	0.33	56.4

* Standard deviation from fraction folded fit using KaleidaGraph is 0.5 for all samples, NA = not applicable.

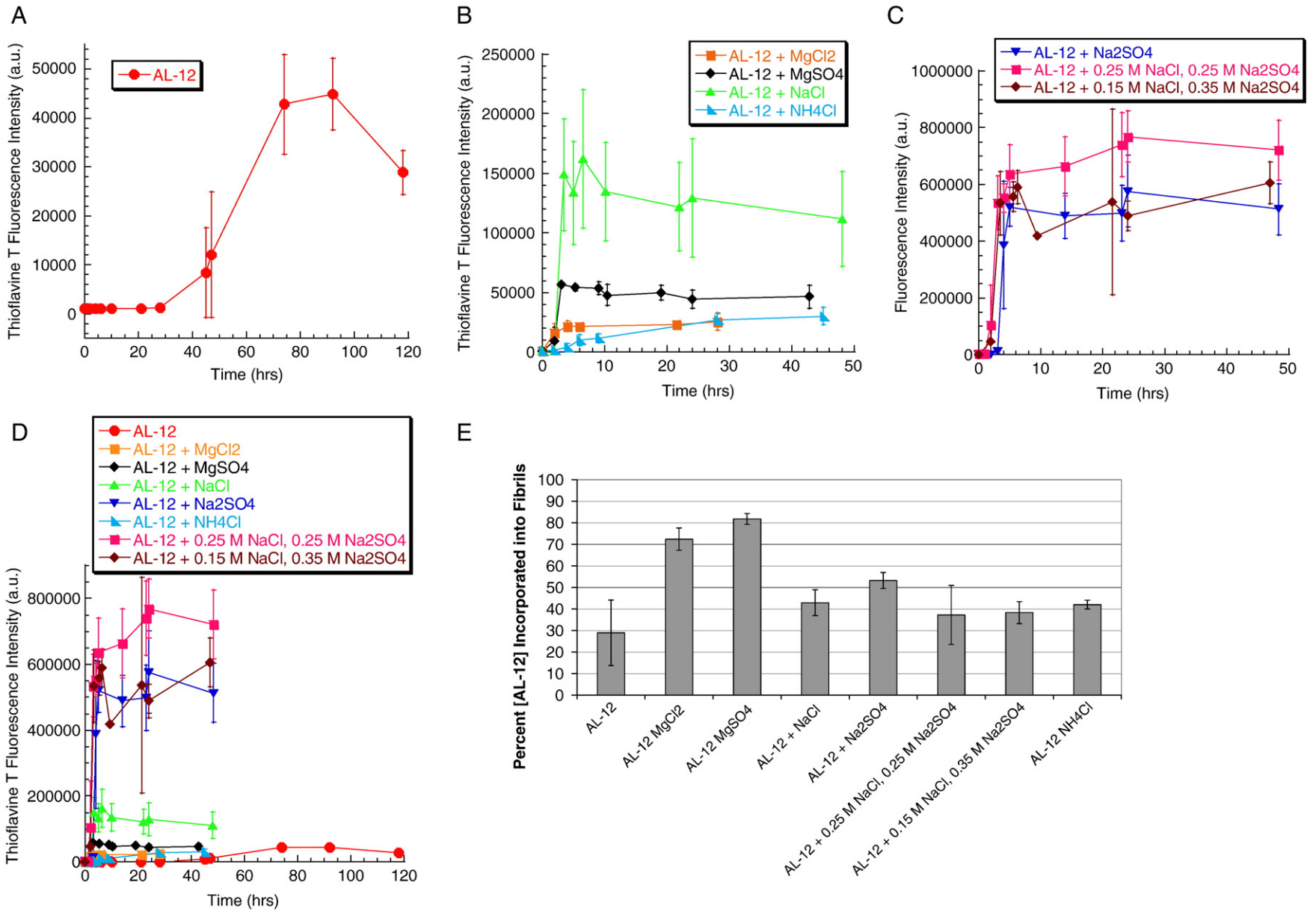

Fig. 3. AL-12 fibril formation followed by ThT fluorescence of samples at their T_m. Excitation wavelength at 450 nm, emission followed from 470–530 nm with maximum fluorescence enhancement at 485 nm (plotted) for each sample. Samples were set up in triplicate with averages plotted. A. AL-12; B. AL-12 + $MgCl_2$, AL-12 + $MgSO_4$, AL-12 + NaCl, AL-12 + NH_4Cl; C. AL-12 + Na_2SO_4, AL-12 + 0.25 M NaCl, 0.25 M Na_2SO_4, AL-12 + 0.15 M NaCl, 0.35 M Na_2SO_4; D. Data from Fig. 4A–C shown in the same plot; E. Percent concentration of AL-12 incorporated into fibrils. Protein concentration in the supernatant was determined for each reaction. Experimental conditions: 10 mM Tris HCl pH 7.4 buffer ±0.5 M Salts (unless noted), 5 μM ThT, 0.02% NaN_3, continuous agitation at 300 nm, at their T_m (59 °C for SO_4^{2-}, 52 °C for Cl^-, 59 °C for Cl^-, SO_4^{2-}, 55 °C for NH_4^+).

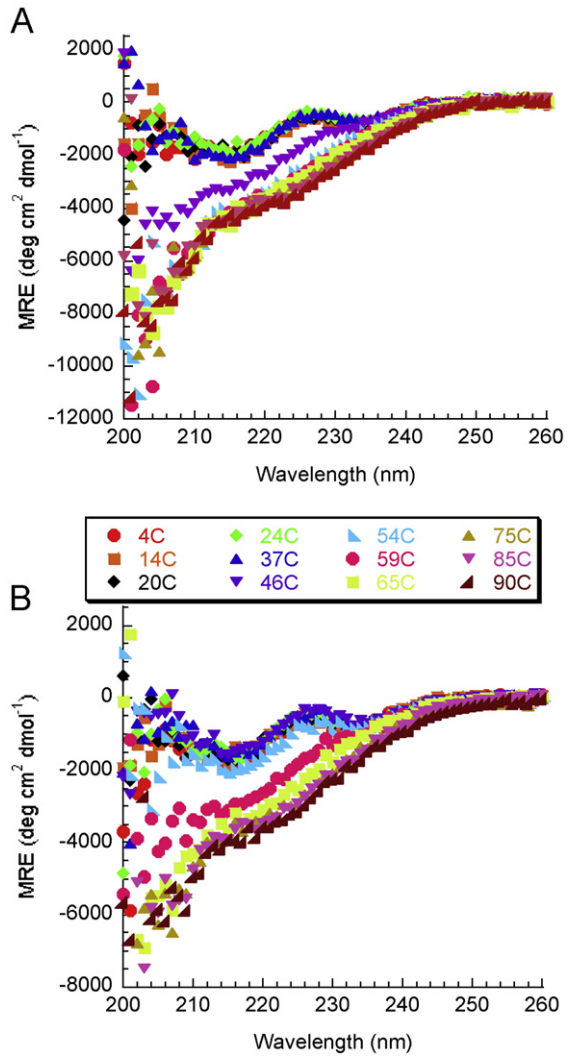

Fig. 4. Structural changes in the β sheet conformation of AL-12±0.5 M Na_2SO_4 at different temperatures. Far UV-CD spectra showed partially unfolded protein in at the T_m. A. AL-12, B. AL-12+0.5 M Na_2SO_4. Experimental conditions: 20 μM protein in 10 mM Tris HCl pH 7.4 buffer. The protein was incubated at different temperatures for 15 min before acquiring data.

salts have on fibril formation. SO_4^{2-} appears to have the largest enhancement in all three areas and Mg^{2+} has the largest effect on amyloid yield. The effect of anions in amyloid formation is in agreement with Hofmeister series for AL-12.

We recorded Far UV-CD spectra at different temperatures to determine the global structure of AL-12 under amyloid forming conditions (T_m) in the presence and absence of Na_2SO_4. AL-12 maintains all of its β sheet structure at low temperatures (including 37 °C) until it reaches its T_m (46 °C) at pH 7.4, at which point it begins to lose its secondary structure and the spectrum broadens, the minimum shifts to 215 nm, and a new minimum at 204 nm appears (Fig. 4A). This spectrum broadening and minimum shift is also seen with the addition of 0.5 M Na_2SO_4 at its T_m (59 °C) in Fig. 4B. At higher temperatures where the protein is unfolded, the spectra maintain residual structure with a more dominant random coil conformation represented by the minimum at 200 nm. This data shows that under amyloid fibril formation conditions in the presence and absence of SO_4^{2-}, AL-12 is partially folded.

4. Discussion

Our study shows that the selected salts did not affect the secondary structure of AL-12 (Fig. 2A), but significantly increased the thermodynamic stability of the protein (Fig. 2B) following the pattern established in the Hofmeister series. All salts promoted amyloid fibril formation with the most enhancement observed with SO_4^{2-} and Mg^{2+} (Fig. 3 and Supplemental Fig. 3).

Apetri and Surewicz have reported the effect of salts on the thermodynamic stability of the human prion protein (huPrP90-231) [21]. Their chemical unfolding studies with urea showed that at low salt concentrations (below ~50 mM), all salts tested significantly reduced thermodynamic stability of the protein. However, at higher salt concentrations (up to 200 mM), the destabilizing effect was gradually reversed, and the salts behaved according to their ranking in the Hofmeister series. In our study, SO_4^{2-} is the most stabilizing salt tested increasing the T_m of AL-12 by 13.2 °C. Anions (SO_4^{2-}, HPO_4^-, Cl^-) significantly affected the thermodynamic stability of AL-12. Cations (NH_4^+ Na^+, Mg^{2+}) did not affect the stability of the protein significantly unless they were paired with SO_4^{2-}. As was reported for the prion protein [21], the stabilizing effect of the anions studied on AL-12 was in good agreement with the rankings of the Hofmeister series at 0.5 M salt concentration. The salts studied have different ionic strengths at 0.5 M ranging from 2.0 for $MgSO_4$ down to 0.5 for NaCl and NH_4Cl (Table 1). At ionic strength of 1, the cations have a larger effect on the stability of the protein than what was observed at 0.5 M salt concentration (Supplemental Fig. 1, Table 1).

As we mentioned in the Introduction, different salts and in particular SO_4^{2-} has been shown to promote amyloid formation for a number of proteins such as AL-09, protein G B1 domain I6T53 variant, β2-microglobulin, α-synuclein and Aβ(1-40) [9–24]. Amyloid formation is also promoted by GAGs which are highly sulfated polysaccharides. It has been reported that the GAG sulfate content is essential to enhance amyloid formation for islet amyloid polypeptide (amylin) [29]. Previous studies in our laboratory have shown that GAGs promote amyloid formation for AL-09. We have also shown that dextran sulfate promotes amyloid formation while dextran has a more neutral effect, suggesting that the SO_4^{2-} content plays a role in this process [9]. It is conceivable that the amyloid formation enhancement observed with SO_4^{2-} is somehow mimicking what is happening in the extracellular matrix with the sulfated GAGs. Mg^{2+} reactions had the highest amyloid yield in our study, possibly due to contribution of this cation in salting-in effects during the aggregation process.

Previous work from our laboratory showed that AL-09 retains some folded structure under amyloid fibril formation conditions (0.5 M Na_2SO_4, 49 °C) [9]. This structure is very similar to the structure we observed for AL-12 (Fig. 4), with a minimum around 215 nm. Raman et al. followed Far UV-CD structure of β2-microglobulin in the presence of 3 mM Na_2SO_4 at pH 2.5, 37 °C (fibril growth favored conditions) and found that the presence of SO_4^{2-} changes β2-microglobulin structure from random coil in the absence of SO_4^{2-} to a structured conformation with two minima around 215 nm and 204 nm [11]. Interestingly, AL-12 also shows a minimum around 204 nm, although our data with 0.5 M Na_2SO_4 is noisy in this region. These results suggest that β2-microglobulin, AL-09 and AL-12, all immunoglobulin proteins, may populate a similar intermediate conformation under fibril forming conditions, regardless of their sequence differences.

5. Conclusions

In this study, we have shown for the first time a direct correlation between protein stability and amyloid formation enhancement by salts from the Hofmeister series. Our study emphasizes the importance of the effect of ionic species in the protein bound water properties and downplays the role of specific interactions between the protein and ionic species such as sulfated glycosaminoglycans. Studies determining the role of sulfated GAGs in AL-12 protein stability, intermediate stabilization and fibril formation are currently underway in our laboratory.

Acknowledgments

We thank Roshini Abraham for providing us with the cDNA for AL-12, Whyte Owen for insight about the Hofmeister series, Grazia Isaya, Heather Thompson and the Ramirez-Alvarado lab for helpful discussions. This study was supported by NIH GM071514, American Heart Association SDG 063007N, and the Mayo Foundation.

Appendix A. Supplementary data

Supplementary data associated with this article can be found, in the online version, at doi:10.1016/j.bpc.2008.02.019.

References

[1] M.R. Hurle, L.R. Helms, L. Li, W. Chan, R. Wetzel, A role for destabilizing amino acid replacements in light-chain amyloidosis, Proc. Natl. Acad. Sci. U. S. A. 91 (1994) 5446–5450.
[2] R. Wetzel, Domain stability in immunoglobulin light chain deposition disorders, Adv. Protein. Chem. 50 (1997) 183–242.
[3] F.J. Stevens, Four structural risk factors identify most fibril-forming kappa light chains, Amyloid 7 (2000) 200–211.
[4] J. Wall, M. Schell, C. Murphy, R. Hrncic, F.J. Stevens, A. Solomon, Thermodynamic instability of human lambda 6 light chains: correlation with fibrillogenicity. Biochemistry 38 (1999) 14101–14108.
[5] C. Ionescu-Zanetti, R. Khurana, J.R. Gillespie, J.S. Petrick, L.C. Trabachino, L.J. Minert, S.A. Carter, A.L. Fink, Monitoring the assembly of Ig light-chain amyloid fibrils by atomic force microscopy, Proc. Natl. Acad. Sci. U. S. A. 96 (1999) 13175–13179.
[6] D.P. Davis, R. Raffen, J.L. Dul, S.M. Vogen, E.K. Williamson, F.J. Stevens, Y. Argon, Inhibition of amyloid fiber assembly by both BiP and its target peptide, Immunity 13 (2000) 433–442.
[7] R. Khurana, J.R. Gillespie, A. Talapatra, L.J. Minert, C. Ionescu-Zanetti, I. Millett, A.L. Fink, Partially folded intermediates as critical precursors of light chain amyloid fibrils and amorphous aggregates, Biochemistry 40 (2001) 3525–3535.
[8] M. Zhu, S. Han, F. Zhou, S.A. Carter, A.L. Fink, Annular oligomeric amyloid intermediates observed by in situ atomic force microscopy, J. Biol. Chem. 279 (2004) 24452–24459.
[9] R.W. McLaughlin, J.K. De Stigter, L.A. Sikkink, E.M. Baden, M. Ramirez-Alvarado, The effects of sodium sulfate, glycosaminoglycans, and Congo red on the structure, stability, and amyloid formation of an immunoglobulin light-chain protein, Protein. Sci. 15 (2006) 1710–1722.
[10] M. Ramirez-Alvarado, M.J. Cocco, L. Regan, Mutations in the B1 domain of protein G that delay the onset of amyloid fibril formation in vitro, Protein. Sci. 12 (2003) 567–576.
[11] B. Raman, E. Chatani, M. Kihara, T. Ban, M. Sakai, K. Hasegawa, H. Naiki, C.M. Rao, Y. Goto, Critical balance of electrostatic and hydrophobic interactions is required for beta 2-microglobulin amyloid fibril growth and stability, Biochemistry 44 (2005) 1288–1299.
[12] A.T. Alexandrescu, Amyloid accomplices and enforcers, Protein. Sci. 14 (2005) 1–12.
[13] F.T. Bosman, I. Stamenkovic, Functional structure and composition of the extracellular matrix, J. Pathol. 200 (2003) 423–438.
[14] A.D. Snow, R. Kisilevsky, Temporal relationship between glycosaminoglycan accumulation and amyloid deposition during experimental amyloidosis. A histochemical study. Lab. Invest. 53 (1985) 37–44.
[15] J.A. Cohlberg, J. Li, V.N. Uversky, A.L. Fink, Heparin and other glycosaminoglycans stimulate the formation of amyloid fibrils from alpha-synuclein in vitro, Biochemistry 41 (2002) 1502–1511.
[16] R. Kisilevsky, W.A. Szarek, J.B. Ancsin, E. Elimova, S. Marone, S. Bhat, A. Berkin, Inhibition of amyloid A amyloidogenesis in vivo and in tissue culture by 4-deoxy analogues of peracetylated 2-acetamido-2-deoxy-alpha- and beta-D-glucose: implications for the treatment of various amyloidoses, Am. J. Pathol. 164 (2004) 2127–2137.
[17] J.B. Ancsin, Amyloidogenesis: historical and modern observations point to heparan sulfate protoglycans as a major culprit, Amyloid 10 (2003) 67–79.
[18] M.G. Cacace, E.M. Landau, J.J. Ramsden, The Hofmeister series: salt and solvent effects on interfacial phenomena, Q Rev Biophys 30 (1997) 241–277.
[19] R.L. Baldwin, How Hofmeister ion interactions affect protein stability, Biophys. J. 71 (1996) 2056–2063.
[20] J.H. Johnston, The surface tension of protein solutions. Part III, Biochem. J. 21 (1927) 1314–1328.
[21] A.C. Apetri, W.K. Surewicz, Atypical effect of salts on the thermodynamic stability of human prion protein, J. Biol. Chem. 278 (2003) 22187–22192.
[22] J.M. Broering, A.S. Bommarius, Evaluation of Hofmeister effects on the kinetic stability of proteins, J. Phys. Chem. 109 (2005) 20612–20619.
[23] L.A. Munishkina, J. Henriques, V.N. Uversky, A.L. Fink, Role of protein–water interactions and electrostatics in alpha-synuclein fibril formation, Biochemistry 43 (2004) 3289–3300.
[24] K. Klement, K. Wieligmann, J. Meinhardt, P. Hortschansky, W. Richter, M. Fandrich, Effect of different salt ions on the propensity of aggregation and on the structure of Alzheimer's Ab(1-40) amyloid fibrils, JMB 373 (2007) 1321–1333.
[25] R.S. Abraham, S.M. Geyer, T.L. Price-Troska, C. Allmer, R.A. Kyle, M.A. Gertz, R. Fonseca, Immunoglobulin light chain variable (V) region genes influence clinical presentation and outcome in light chain-associated amyloidosis (AL), Blood 101 (2003) 3801–3808.
[26] C.N. Pace, M. Scholtz, Protein structure, a practical approach, in: T.E. Creighton (Ed.), Measuring the Conformational Stability of a Protein, 1st ed, Oxford University Press, New York, 1997, p. 383.
[27] B. Albinsson, B. Nordeen, Excited-state properties of the indole chromophore: electronic transition moment directions from linear dichroism measurements: effect of methyl and methoxy substitutents. J. Phys. Chem 96 (1992) 6204–6212.
[28] M. Ramirez-Alvarado, J.S. Merkel, L. Regan, A systematic exploration of the influence of the protein stability on amyloid fibril formation in vitro, Proc. Natl. Acad. Sci. U. S. A. 97 (2000) 8979–8984.
[29] G.M. Castillo, J.A. Cummings, W. Yang, M.E. Judge, M.J. Sheardown, K. Rimvall, J. Bondo Hansen, A.D. Snow, Sulfate content and specific glycosaminoglycan backbone of perlecan are critical for perlecan's enhancement of islet amyloid polypeptide (amylin) fibril formation, Diabetes 47 (1998) 612–620.
[30] N.L. Jarvis, M.A. Scheiman, Surface potentials of aqueous electrolyte solutions, J. Phys. Chem. 72 (1968) 74–78.
[31] P.K. Nandi, D.R. Robinson, The effects of salts on the free energies of nonpolar groups in model peptides, J. Am. Chem. Soc. 94 (1972) 1308–1315.